Pushed fronts in a Fisher-KPP-Burgers system using geometric desingularization

Matt Holzer, Matthew Kearney, Samuel Molseed, Katie Tuttle and David Wigginton

Department of Mathematical Sciences, George Mason University, Fairfax, VA, USA

December 13, 2022

Abstract

We study traveling fronts in a system of one dimensional reaction-diffusion-advection equations motivated by problems in reactive flows. In the limit as a parameter tends to infinity, we construct the approximate front profile and determine the leading order expansion for the selected wavespeed. Such fronts are often constructed as transverse intersections of stable and unstable manifolds of the traveling wave differential equation. However, a re-scaling of the dependent variable leads to a lack of hyperbolicity for one of the end states making the definition of one such manifold unclear. We use geometric blow-up techniques to recover hyperbolicity and following an analysis of the blown up vector field are able to show the existence of a traveling front with a leading order expansion of its speed.

Keywords: pushed fronts, geometric singular perturbation theory, geometric desingularization

1 Introduction

The following system of reaction-diffusion-advection equations was recently introduced in [6],

$$\begin{aligned} T_t &= T_{xx} - (uT)_x + T(1-T) \\ u_t &= \nu u_{xx} - uu_x + \rho T(1-T). \end{aligned} \tag{1.1}$$

Here $T(t,x)$ models the temperature of a fluid and $u(t,x)$ represents the velocity of that fluid. The reaction term in the T component introduces growth of the temperature field due to the occurrence of a chemical reaction. The temperature increase also induces growth in the velocity profile with some proportionality constant ρ. Both temperature and velocity also are influenced by diffusion and advection. System (1.1) gives rise to traveling front solutions. Motivated by similar systems of coupled fluid and reaction-diffusion equations such as [8, 22] the goal of [6] is to understand how

coupling between the two variables affects the speed of these fronts. A more detailed description of model (1.1) and its relation to other models of reactive flow can be found in [6].

The authors in [6] study traveling fronts for (1.1) with a particular interest in how the speeds of these fronts depend on the parameters ρ and ν. The purpose of this paper is to study fronts in the inviscid problem ($\nu = 0$) and in the limit as $\rho \to \infty$. When $\nu = 0$ the traveling wave equations for (1.1) as a system of three first order ordinary differential equations. These systems have a conserved quantity which reduces the traveling wave equation to the following planar system, see [6]

$$\begin{aligned} \frac{dT}{dx} &= -\tilde{c}T + UT + \frac{1}{2\rho}U(2\tilde{c} - U) \\ \frac{dU}{dx} &= \frac{\rho}{U - \tilde{c}}T(1 - T). \end{aligned} \tag{1.2}$$

Traveling fronts of (1.1) correspond to heteroclinic orbits of (1.2) that connect the PDE stable state $(1, \tilde{c} + \rho - \sqrt{\tilde{c}^2 + \rho^2})$ to the PDE unstable state $(0, 0)$. As is typical of fronts propagating into unstable states these fronts exist for a continuum of speeds $\tilde{c}$. Of particular interest is the front that is selected by compactly supported initial conditions. This front is often referred to as the critical front and its speed is known as the critical (or selected) spreading speed. Typically the critical front can be classified as being of one of two types: pulled or pushed. Pulled fronts are driven by the instability ahead of the front interface and their spreading speed equals that of compactly supported initial conditions for the equation linearized near the unstable steady state. Pushed fronts are driven by nonlinear effects behind the front interface propagate at (typically, see [17]) faster-than-linear speeds.

Determining the front selected by compactly supported initial data is associated to stability properties of the fronts; see [4, 9, 23]. Pulled fronts have essential spectrum that touches the imaginary axis in an optimally chosen exponentially weighted function space while pushed fronts have a zero translational eigenvalue and stable essential spectrum in the weighted space. This translational eigenvalue has a eigenfunction given by the derivative of the front profile and so for this function to be in the weighted space requires strong exponential decay of the front. When considering heteroclinic orbits in (1.2) this will mean that we will seek heteroclinic orbits with the strongest possible decay to the origin. We refer the interested reader to [23] for an in-depth discussion of pushed and pulled fronts and we note recent work on pushed and pulled fronts and the transition between them; see [2, 3].

The explicit construction of heteroclinic orbits for nonlinear ordinary differential equations is difficult. Most examples where pushed invasion speeds can be calculated involve scalar equations where explicit solutions can be obtained as in the classical Nagumo's equation; see [14]. For systems of reaction-diffusion equations the situation is more challenging still – the most promising avenue is when one or more parameters in the system are asymptotically small (or large). In these situations, singular perturbation theory (see [12, 20]) can be employed to construct solutions and wavespeed estimates are sometimes possible by analyzing a reduced planar system; see for example [15, 17, 18].

Among other results, the following estimate of the critical speed in the limit as $\rho \to \infty$ was obtained

in [6].

Theorem 1.1. *[6] System (1.1) with $\nu = 0$ has traveling front solutions connecting the stable state $(1, \tilde{c} + \rho - \sqrt{\tilde{c}^2 + \rho^2})$ to $(0, 0)$ for any $\tilde{c} \geq \tilde{c}^*(\rho)$. These fronts are monotonic and for $\rho \to \infty$ the critical speed $\tilde{c}^*(\rho)$ satisfies*

$$\sqrt[3]{\frac{3}{2}} \leq \liminf_{\rho\to\infty} \frac{\tilde{c}^*(\rho)}{\rho^{1/3}} \leq \limsup_{\rho\to\infty} \frac{\tilde{c}^*(\rho)}{\rho^{1/3}} \leq \sqrt{3} \tag{1.3}$$

Numerical estimates of the critical speed were obtained in [6] using methods from [5] and suggest that the critical speed should scale like the lower bound in (1.3). The purpose of the current research is to refine the estimate in Theorem 1.1 and show that the critical speed does in fact scale with $\sqrt[3]{\frac{3\rho}{2}}$ as $\rho \to \infty$.

To this end, we make the following changes of coordinates: $\rho = \frac{1}{\varepsilon^3}$, $c = \tilde{c}/\varepsilon$, $W = \varepsilon U$ and $X = \varepsilon x$. Then (1.2) is transformed to the following system of equations with small parameter ε,

$$\begin{aligned} \frac{dT}{dX} &= -cT + WT + \frac{1}{2}W\varepsilon^2(2c - W) \\ \frac{dW}{dX} &= \frac{1}{W - c}T(1 - T). \end{aligned} \tag{1.4}$$

A general framework for proving the existence of traveling waves (i.e. heteroclinic orbits) in singularly perturbed systems is as follows; see for example [20]. One first sets the small parameter to zero and identifies a heteroclinic orbit in this singular limit. In the case of (1.2) this heteroclinic involves the intersection of two one dimensional manifolds. As such, the system is not structurally stable and the heteroclinic is not expected to persist when $\varepsilon \neq 0$. However, if the system has a parameter (c in our case) then one can add the parameter as a variable to increase the dimension of the system and construct two dimensional center-stable and center-unstable manifolds. If these manifolds intersect transversely and depend smoothly on ε then the transverse intersection will persist for $\varepsilon > 0$ and the existence of a heteroclinic follows without having to delve into the particular manner in which ε appears in the equations.

The primary complication occurring in (1.4) is that the heteroclinic in the singular limit involves a connection to a non-hyperbolic fixed point. Thus, even the persistence of this fixed point when $\varepsilon \neq 0$ is not apparent and it is not possible to define stable or unstable manifolds of this fixed point without explicitly considering ε dependent terms. To overcome this issue we will apply geometric desingularization techniques to blow-up the non-hyperbolic fixed point and regain hyperbolicity. We refer the reader to [10, 21] for a description of the method. Related to the problem of front propagation: blow-up has been used to compute correction to wavespeeds due to cutoff in reaction terms; see [11]. We also point to other examples where re-scalings of the dependent variables lead to a lack of hyperbolicity – see for example [7, 13, 16].

The main result of this paper is the following.

Theorem 1.2. *Let $\nu = 0$ in (1.1). Then there exists a $\rho_0 > 0$ such that for any $\rho > \rho_0$ there exists a traveling front solution of (1.1) connecting the stable state $(1, \tilde{c} + \rho - \sqrt{\tilde{c}^2 + \rho^2})$ to $(0, 0)$ with speed $\tilde{c}^*(\rho)$ such that*

(i) the front is monotone decreasing and has steep exponential decay in the sense that

$$|(T^*(x), Q^*(x))| \leq Ce^{-\tilde{c}^*(\rho)x/2} \text{ as } x \to \infty$$

(ii) the speed $\tilde{c}^*(\rho)$ *satisfies* $\lim_{\rho\to\infty} \frac{\tilde{c}^*(\rho)}{\sqrt[3]{\rho}} = \sqrt[3]{\frac{3}{2}}$

The rest of the paper is dedicated to proving this Theorem and is organized as follows. In Section 2 we change coordinates in the traveling wave equation (1.4) and collect some facts about this transformed system. In Section 3 we set $\varepsilon = 0$ and obtain a candidate traveling front. This front involves a heteroclinic orbit involving a non-hyperbolic fixed point. In Section 4 we apply geometric desingularization techniques to track invariant manifolds near this point. We conclude in Section 5 with the proof of Theorem 1.2.

2 Preliminaries

We begin our analysis by removing the singularity that occurs in (1.4) at $W = c$. This is accomplished by rescaling the independent variable so that the right hand side of (1.4) is multiplied by the non-zero factor $c - W$. Since we are interested in the region where $W < c$ then this quantity is always positive and does not reverse the direction of the flow. We then arrive at the system

$$\begin{aligned} \dot{T} &= -T(W-c)^2 - \frac{1}{2}W\varepsilon^2(2c-W)(W-c) \\ \dot{W} &= -T(1-T). \end{aligned} \tag{2.1}$$

System (2.1) has fixed points at $(0,0)$, $(1,c)$ and $(1, w_\pm(\varepsilon))$ where $w_\pm(\varepsilon)$ are roots of the quadratic polynomial

$$h(w) = w - c + \frac{1}{2}\varepsilon^2 w(2c-w),$$

which can be expressed as

$$w_\pm(\varepsilon) = c + \frac{1}{\varepsilon^2} \pm \frac{1}{\varepsilon^2}\sqrt{1+\varepsilon^4 c^2}.$$

We are interested in fronts connecting $(1, w_-(\varepsilon))$ to $(0,0)$ and note that

$$w_-(\varepsilon) = c - \varepsilon^2\frac{c^2}{2} + \mathcal{O}(\varepsilon^4). \tag{2.2}$$

It will be consequential later that $w_-(\varepsilon) < c$ and $w_-(\varepsilon) \to c$ as $\varepsilon \to 0$.

The linearization of (2.1) at $(0,0)$ has two negative eigenvalues

$$\mu_\pm(c,\varepsilon) = -\frac{c^2}{2} \pm \frac{c^2}{2}\sqrt{1+4\varepsilon^2}. \tag{2.3}$$

The linearization at $(1, w_-(\varepsilon))$ is

$$\begin{pmatrix} -(w_-(\varepsilon)-c)^2 & -(w_-(\varepsilon)-c)h'(w_-(\varepsilon)) \\ 1 & 0 \end{pmatrix}.$$

Since the trace is negative and the determinant is negative (note $h'(w_-(\varepsilon)) > 0$) we then see that the fixed point $(1, w_-(\varepsilon))$ is a saddle with one stable and one unstable eigenvalue. Regrettably, both these eigenvalues are close to zero so that when $\varepsilon = 0$ the fixed point is no longer hyperbolic and its linearization is nilpotent. We emphasize that this lack of hyperbolicity can be traced to the fact that as $\varepsilon \to 0$ the fixed point at $(1, w_-(\varepsilon))$ coalesces with the fixed point at $(1, c)$ yielding a non-hyperbolic fixed point.

Nonetheless, for any $0 < \varepsilon \ll 1$ the unstable manifold $W^u(1, w_-(\varepsilon))$ is well defined and can be written as a graph $(T, h_u(c, \varepsilon, T))$. Likewise, for c fixed and $0 < \varepsilon \ll 1$ the origin has a one dimensional strong stable manifold $W^{ss}(0, 0)$ which can also be expressed as a graph $(T, h_s(c, \varepsilon, T))$. We then define the mismatch function

$$\Phi(c, \varepsilon) = h_s\left(c, \varepsilon, \frac{1}{2}\right) - h_u\left(c, \varepsilon, \frac{1}{2}\right). \tag{2.4}$$

We will establish the following result.

Theorem 2.1. *We have the following*

- *The function $\Phi(c, \varepsilon)$ is continuously differentiable in both c and ε.*
- $\Phi\left(\sqrt[3]{\frac{3}{2}}, 0\right) = 0$
- $\partial_c \Phi\left(\sqrt[3]{\frac{3}{2}}, 0\right) \neq 0$

By an application of the Implicit Function Theorem, Theorem 2.1 will then imply Theorem 1.2.

Remark 2.2. *Theorem 2.1 can also be interpreted as a statement about transversality of manifolds. If we append the trivial equation $c' = 0$ to (2.1) then there exist a two-dimensional center-strong stable manifold of the origin and a two dimensional center-unstable manifold for $(1, w_-(\varepsilon))$. The condition (ii) in Theorem 2.1 then says that these manifolds intersect and condition (iii) implies that this intersection is transverse. Smooth dependence on ε then implies that this transverse intersection will persist for $\varepsilon \neq 0$.*

3 Reduction to the singular limit $\varepsilon = 0$

In this section we study (2.1) with $\varepsilon = 0$ and construct a heteroclinic orbit that connects the fixed point $(1, c)$ to the one at $(0, 0)$. With $\varepsilon = 0$ the system reduces to

$$\begin{aligned} \dot{T} &= -T(W - c)^2 \\ \dot{W} &= -T(1 - T). \end{aligned} \tag{3.1}$$

For $0 < T < 1$ solutions of this system are graphs with respect to the variable T and their solution curves obey the scalar equation

$$\frac{dW}{dT} = \frac{1 - T}{(W - c)^2}. \tag{3.2}$$

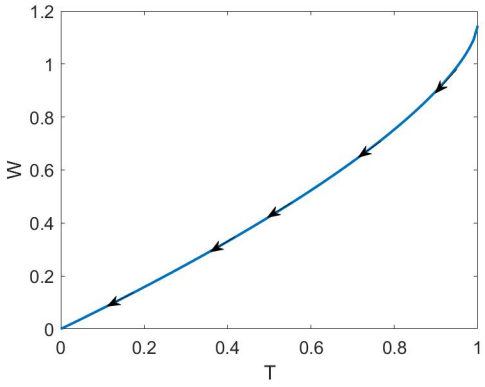

Figure 1: *The heteroclinic orbit obtained for the reduced ($\varepsilon = 0$) system connecting the fixed point $(1, c)$ to the origin with $c = c^*(0) = \sqrt[3]{\frac{3}{2}}$.*

This equation is separable and can be integrated to find solution curves that satisfy

$$\frac{1}{3}(W - c)^3 = T - \frac{T^2}{2} + k \tag{3.3}$$

where k is a constant of integration.

For the curve in (3.3) to pass through the origin it is required that $k_0 = -\frac{c^3}{3}$. For the curve to pass through the point $(1, c)$ it is required that $k_1 = -\frac{1}{2}$. Therefore, the curves intersect if and only if $c = c^*(0)$ with

$$c^*(0) = \sqrt[3]{\frac{3}{2}}. \tag{3.4}$$

A plot of this solution curve is provided in Figure 1.

For future reference we define the functions

$$g_s(c, T) = c + \sqrt[3]{3T - \frac{3}{2}T^2 - c^3},$$

which gives the W component of the graph of the solution curve passing through the origin while we define

$$g_u(c, T) = c + \sqrt[3]{3T - \frac{3}{2}T^2 - \frac{3}{2}}.$$

We make note of the following fact.

Lemma 3.1. *For any $T > 0$*

$$\frac{\partial}{\partial c}\left(g_s(c, T) - g_u(c, T)\right) \neq 0.$$

Proof. We compute

$$\frac{\partial}{\partial c}\left(g_s(c, T) - g_u(c, T)\right) = -\frac{c^2}{(3T - \frac{3}{2}T^2 - c^3)^{2/3}} \neq 0$$

□

4 A quasi-homogeneous blow-up of the nilpotent fixed point $(1, c)$

When $\varepsilon = 0$ the fixed point $(1, c)$ is not hyperbolic. To prove Theorem 1.2 we need to show that the unstable manifold of $(1, w_-(\varepsilon))$ is $o(1)$ close to the heteroclinic orbit computed in Section 3. To do this we will use geometric desingularization to blow-up and then desingularize the flow near this fixed point.

To begin, we first transform the fixed point at $(1, c)$ to the origin using

$$\tilde{W} = W - c, \quad \tilde{T} = T - 1,$$

from which we obtain the system of equations (appending an equation for the parameter ε)

$$\begin{aligned} \tilde{T}' &= -\tilde{W}^2(\tilde{T}+1) - \frac{1}{2}\tilde{W}\varepsilon^2(c^2 - \tilde{W}^2) \\ \tilde{W}' &= \tilde{T}(\tilde{T}+1) \\ \varepsilon' &= 0. \end{aligned} \tag{4.1}$$

The linearization at the origin is nilpotent with Jacobian

$$Df(0,0,0) = \begin{pmatrix} 0 & 0 & 0 \\ 1 & 0 & 0 \\ 0 & 0 & 0 \end{pmatrix}.$$

The goal of this section is to blow-up the non-hyperbolic origin in (4.1) to a sphere where – after desingularizing by a re-scaling of the independent variable – the flow in a neighborhood of the origin can be analyzed by studying the flow on the sphere. In the simplest case, blow-up techniques involve viewing (4.1) in spherical coordinates (ρ, θ, ϕ) where after desingularizing one obtains non-trivial dynamics on the surface of the sphere ($\rho = 0$). However, use of such coordinates for (4.1) reveals fixed points on the surface of the sphere which remain non-hyperbolic.

We therefore employ a quasi-homogeneous blow-up where different scalings are given to different variables; see [1, 10, 19, 21] for examples and a general discussion. The change of variables that we employ is defined as

$$\psi : \mathbb{S}^2 \times [0, \infty) \to \mathbb{R}^3, \quad \psi\left(\bar{T}, \bar{W}, \bar{\varepsilon}, r\right) = \left(r^3\bar{T}, r^2\bar{W}, r\bar{\varepsilon}\right),$$

where $(\bar{T}, \bar{W}, \bar{\varepsilon}) \in \mathbb{S}^2$. We comment on the choice of weights. Since the fixed point $w_-(\varepsilon)$ depends quadratically on ε then it is natural that the weight for the $\tilde{W}$ component should be squared relative to the weight for ε. The cubic scaling for the $\tilde{T}$ component can be determined as follows. Let $\tilde{T} = r^\alpha\bar{T}$. Then the leading order terms on the right hand side of (4.1) scale with r^4 for $\tilde{T}'$ equation and r^α for the $\tilde{W}'$ equation. Thus the scaling of the two equations match only if $4 - \alpha = \alpha - 2$ from which $\alpha = 3$ is determined.

The variables $\left(\bar{W},\bar{T},\bar{\varepsilon}\right) \in \mathbb{S}^2$ could be expressed in terms of spherical coordinates; however in practice it is easier to use various coordinate charts in which to view the dynamics. We will employ the following two charts for our analysis

$$\begin{aligned} K_\varepsilon: &\qquad \tilde{T} = r_1^3 T_1,\ \tilde{W} = -r_1^2 W_1,\ \varepsilon = r_1 \\ K_W: &\qquad \tilde{T} = r_2^3 T_2,\ \tilde{W} = -r_2^2,\ \varepsilon = r_2\varepsilon_2, \end{aligned}$$

where we will assume $r_{1,2} \geq 0$, $W_1 \geq 0$, $T_{1,2} \leq 0$ and $\varepsilon_2 \geq 0$.

Transition maps between the two charts are

$$r_2 = r_1 W_1^{1/2},\ T_2 = \frac{T_1}{W_1^{3/2}},\ \varepsilon_2 = \frac{1}{W_1^{1/2}} \tag{4.2}$$

$$T_1 = \frac{T_2}{\varepsilon_2^3},\ W_1 = \frac{1}{\varepsilon_2^2},\ r_1 = r_2\varepsilon_2. \tag{4.3}$$

4.1 Chart K_ε

Chart K_ε is referred to as the re-scaling chart. Equation (4.1) expressed in the coordinates of chart K_ε are

$$\begin{aligned} T_1' &= -r_1 W_1^2\left(1 + r_1^3 T_1\right) + \frac{1}{2} r_1 W_1\left(c^2 - r_1^4 W_1^2\right) \\ W_1' &= -r_1 T_1 - r_1^4 T_1^2 \\ r_1' &= 0. \end{aligned} \tag{4.4}$$

Dividing the right side of the equation by the common factor r_1 through a rescaling of the independent variable we obtain the desingularized equations

$$\begin{aligned} \frac{dT_1}{dt_1} &= -W_1^2\left(1 + r_1^3 T_1\right) + \frac{1}{2} W_1\left(c^2 - r_1^4 W_1^2\right) \\ \frac{dW_1}{dt_1} &= -T_1 - r_1^3 T_1^2 \\ \frac{dr_1}{dt_1} &= 0. \end{aligned} \tag{4.5}$$

The invariant subspace $r_1 = 0$ corresponds to the flow on the surface of the sphere in blown-up coordinates where

$$\begin{aligned} \frac{dT_1}{dt_1} &= -W_1^2 + \frac{c^2}{2} W_1 \\ \frac{dW_1}{dt_1} &= -T_1. \end{aligned} \tag{4.6}$$

Equation (4.6) has fixed points at $(0,0)$ (a center) and at $\left(0, \frac{c^2}{2}\right)$ (a saddle). The saddle fixed point in this chart corresponds to the fixed point $(1, w_-(0))$ while the fixed point at the origin is an

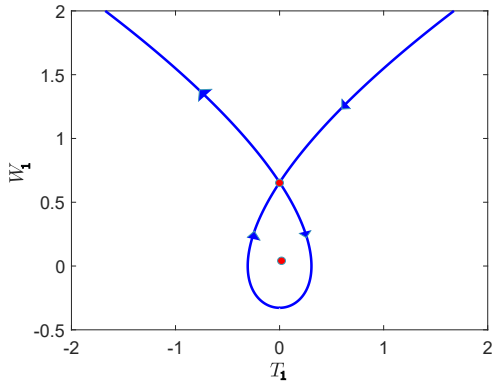

Figure 2: *The dynamics in chart K_ε for $c = \sqrt[3]{\frac{3}{2}}$. The system is Hamiltonian and there exists an explicit expression for the graph of the unstable manifold that exists for $T_1 < 0$.*

artifact of the desingularization that removed the singularity at $(1, c)$ in the original coordinates. Thus, the blow-up technique is able to differentiate between these two fixed points in the limit as $\varepsilon \to 0$ and the fixed point at $(1, w_-(0))$ becomes hyperbolic when viewed in this chart.

System (4.6) is also Hamiltonian with

$$H(T_1, W_1) = \frac{W_1^3}{3} - \frac{c^2}{4}W_1^2 - \frac{T_1^2}{2}.$$

The unstable manifold of $\left(0, \frac{c^2}{2}\right)$ is contained in the level set of $H(T_1, W_1) = -\frac{1}{48}c^6$. This level curve is plotted in Figure 2 for $c = \sqrt[3]{\frac{3}{2}}$.

4.2 Chart K_W

We now consider the dynamics in the chart K_W. Equation (4.1) transformed to the coordinates of this chart are given by

$$\begin{aligned} r_2' &= -\frac{1}{2}r_2^2 T_2 - \frac{1}{2}r_2^5 T_2^2 \\ \varepsilon_2' &= \frac{1}{2}r_2\varepsilon_2 T_2 + \frac{1}{2}r_2^4\varepsilon_2 T_2^2 \\ T_2' &= -r_2(1 + r_2^3 T_2) + \frac{1}{2}r_2\varepsilon_2^2\left(c^2 - r_2^4\right) + \frac{3}{2}r_2 T_2^2 + \frac{3}{2}r_2^4 T_2^3. \end{aligned} \tag{4.7}$$

The vector field can be desingularized by dividing the right side by the common factor r_2 after which (4.7) is transformed to

$$\begin{aligned} \frac{dr_2}{dt_2} &= -\frac{1}{2}r_2 T_2 - \frac{1}{2}r_2^4 T_2^2 \\ \frac{d\varepsilon_2}{dt_2} &= \frac{1}{2}\varepsilon_2 T_2 + \frac{1}{2}r_2^3\varepsilon_2 T_2^2 \\ \frac{dT_2}{dt_2} &= -(1 + r_2^3 T_2) + \frac{1}{2}\varepsilon_2^2\left(c^2 - r_2^4\right) + \frac{3}{2}T_2^2 + \frac{3}{2}r_2^3 T_2^3. \end{aligned} \tag{4.8}$$

Restricting to the invariant subspace $r_2 = 0$ we obtain the system

$$\begin{aligned} \frac{d\varepsilon_2}{dt_2} &= \frac{1}{2}\varepsilon_2 T_2. \\ \frac{dT_2}{dt_2} &= -1 + \frac{1}{2}\varepsilon_2^2 c^2 + \frac{3}{2}T_2^2. \end{aligned} \tag{4.9}$$

This system has four fixed points: $\left(0, \pm\sqrt{\frac{2}{3}}\right)$ and $\left(\pm\sqrt{\frac{2}{c^2}}, 0\right)$. Using (4.3) we see that the fixed point $\left(\sqrt{\frac{2}{c^2}}, 0\right)$ is equivalent to $w_-(0)$ in the original coordinates and $\left(\frac{c^2}{2}, 0\right)$ in the chart K_ε. We make the following observations. First the $\varepsilon_2 = 0$ subspace is invariant and the fixed point $(0, -\sqrt{2/3})$ is stable with eigenvalues $-3\sqrt{2/3}$ and $-\frac{1}{2}\sqrt{2/3}$ (note the $6:1$ resonance).

To analyze the transition map for (4.8) we divide the vector field by the (locally) positive factor $\frac{1}{2}(-T_2 - r_2^3 T_2^2)$ effectively introducing a new independent variable, σ. We then shift the fixed point to the origin $S_2 = T_2 + \sqrt{\frac{2}{3}}$ after which (4.8) takes the form

$$\begin{aligned} \frac{dr_2}{d\sigma} &= r_2 \\ \frac{d\varepsilon_2}{d\sigma} &= -\varepsilon_2 \\ \frac{dS_2}{d\sigma} &= -6S_2 + F(r_2, \varepsilon_2, S_2), \end{aligned} \tag{4.10}$$

for some locally smooth nonlinear function $F(r_2, \varepsilon_2, S_2)$. We now change coordinates. The unstable manifold of $(0, 0, -\sqrt{2/3})$ is contained in the $\varepsilon_2 = 0$ subspace and can be expressed as a graph over the r_2 axis which we denote by $\phi(r_2)$. Then the change of coordinates $Q_2 = S_2 - \phi(r_2)$ straightens the unstable manifold to coincide with the r_2 axis. As a result (4.10) is transformed to

$$\begin{aligned} \frac{dr_2}{d\sigma} &= r_2 \\ \frac{d\varepsilon_2}{d\sigma} &= -\varepsilon_2 \\ \frac{dQ_2}{d\sigma} &= -6Q_2 + Q_2 G_1(r_2, Q_2) + \varepsilon_2 G_2(r_2, \varepsilon_2, Q_2). \end{aligned} \tag{4.11}$$

Here G_1 and G_2 are nonlinear functions that represent the nonlinearity after the change of coordinates. The function $G_1(0,0) = 0$ since it contains only nonlinear terms and $G_2(0,0,0) = 0$ since the linear term ε_2 is absent from (4.11).

For $\kappa > 0$ define the sections Σ_{in} and Σ_{out} as

$$\Sigma_{in} = \{(r_2, \varepsilon_2, S_2) \mid \varepsilon_2 = \kappa\},\ \Sigma_{out} = \{(r_2, \varepsilon_2, S_2) \mid r_2 = \kappa\}.$$

We study the transition map $\pi : \Sigma_{in} \to \Sigma_{out}$.

Lemma 4.1. *Consider initial conditions in Σ_{in} with $r_2 = \varepsilon\Gamma(c, \varepsilon, \kappa)$ and $S_2 = \Omega(c, \varepsilon, \kappa)$ for some smooth functions Γ and Ω. Then if κ is sufficiently small it holds that*

$$\pi(\varepsilon\Gamma(c, \varepsilon, \kappa), \Omega(c, \varepsilon, \kappa)) = (\varepsilon\Gamma(c, \varepsilon), \phi(r_2) + \varepsilon\Xi(c, \varepsilon))$$

for some smooth function $\Xi(c, \varepsilon)$.

Remark 4.2. *The fixed point in (4.11) is hyperbolic and so we could linearize the system by a near-identity change of coordinates using Hartman-Grobman Theorem. Resonances between the eigenvalues limit the smoothness of the conjugacy mapping and, even still, the mere existence of a near-identity conjugacy is not sufficient to obtain the estimates that we desire.*

Proof. Take the integral form of (4.11),

$$\begin{aligned} Q_2(\sigma) &= e^{-6\sigma}Q_2(0) + \int_0^\sigma e^{-6(\sigma-\tau)}Q_2(\tau)G_1\left(\varepsilon\Gamma(c,\varepsilon)e^\tau, Q_2(\tau)\right)\mathrm{d}\tau \\ &+ \kappa\int_0^\sigma e^{-6(\sigma-\tau)}e^{-\tau}G_2\left(\varepsilon\Gamma(c,\varepsilon)e^\tau, \kappa e^{-\tau}, Q_2(\tau)\right)\mathrm{d}\tau. \end{aligned} \tag{4.12}$$

The transition "time" required for the solution to pass from Σ_{in} to Σ_{out} is

$$\sigma^* = \log\left(\frac{\kappa}{\varepsilon\Gamma(c,\varepsilon,\kappa)}\right).$$

We need estimates on the solution of this equation on the interval $[0,\sigma^*]$. Define $\Psi : X \to X$ as the right hand side of (4.12) and let X be the Banach Space

$$X = C^0([0,\sigma^*],\mathbb{R}),\ ||Q||_X = \sup_{0<\sigma<\sigma^*}|e^\sigma Q(\sigma)|.$$

Then for any $Q \in X$ we have

$$|e^\sigma \Psi Q| \leq \left|e^{-5\sigma}Q(0)\right| + \int_0^\sigma e^{-5(\sigma-\tau)}||Q||_X|G_1(\tau)|\mathrm{d}\tau \tag{4.13}$$

$$+ \kappa\int_0^\sigma e^{-5(\sigma-\tau)}|G_2(\tau)|\mathrm{d}\tau. \tag{4.14}$$

Thus

$$||\Psi Q||_X \leq |\Omega(c,\varepsilon,\kappa)| + C_1\kappa||Q||_X + C_2\kappa^2,$$

and $\Psi : X \to X$. Next we show that Ψ is a contraction on X. Consider Q_a and Q_b, both in X. Then

$$|e^\sigma\Psi(Q_a - Q_b)| \leq L_1\kappa\int_0^\sigma e^{-5(\sigma-\tau)}||Q_a - Q_b||_X\mathrm{d}\tau + \kappa L_2\int_0^\sigma e^{-5(\sigma-\tau)}||Q_a - Q_b||_X\mathrm{d}\tau,$$

where L_1 is the Lipschitz constant of G_1 and L_2 is the Lipschitz constant for $G_2(r_2,\varepsilon_2,Q_2) - G_\varepsilon(r_2,\varepsilon_2,0)$. We then have

$$||\Psi(Q_a - Q_b)||_X \leq C\kappa||Q_a - Q_b||_X$$

and Ψ is a contraction for κ sufficiently small.

Now consider the S_2 coordinate of the transition map π. Since $Q_2 \in X$ we have that

$$|Q_2(\sigma^*)| \leq e^{-\sigma^*}||Q_2||_X$$

and thus $Q_2(\sigma^*) = \varepsilon\Xi(c,\varepsilon)$ for some smooth function $\Xi(c,\varepsilon)$. Changing coordinates back to S_2 we obtain the result.

□

4.3 Tracking $W^u(1, w_-(\varepsilon))$ between charts

We now put together the analysis in the two charts above to track $W^u(1, w_-(\varepsilon))$. In the re-scaling chart K_ε the equilibrium point $(1, w_-(\varepsilon))$ is mapped to (for $\varepsilon = 0$) the fixed point $\left(0, \frac{c^2}{2}\right)$. This fixed point is hyperbolic of saddle type and has a one-dimensional unstable manifold. The fixed point and its unstable manifold persist for $\varepsilon > 0$ and sufficiently small. Using the Hamiltonian function in chart K_ε we find that the unstable manifold (when $\varepsilon = 0$) is expressed as the graph

$$T_1 = -\sqrt{\frac{2}{3}W_1^3 - \frac{c^2}{4}W_1^2 + \frac{1}{24}c^6}.$$

By smooth dependence on initial conditions and parameters we have that

$$T_1 = -\sqrt{\frac{2}{3}W_1^3 - \frac{c^2}{4}W_1^2 + \frac{1}{24}c^6} + \varepsilon\Delta(W_1, c, \varepsilon),$$

for some function Δ.

When $W_1 = \frac{1}{\kappa^2}$ then

$$T_1 = -\sqrt{\frac{2}{3}\frac{1}{\kappa^6} - \frac{c^2}{4}\frac{1}{\kappa^4} + \frac{1}{24}c^6} + \varepsilon\Delta\left(\frac{1}{\kappa^2}, c, \varepsilon\right).$$

Transforming to chart K_W using (4.3) then we have $\varepsilon_2 = \kappa$, $r_2 = \varepsilon\kappa$ and

$$T_2 = -\sqrt{\frac{2}{3} - \frac{c^2}{4}\kappa^2 + \frac{1}{24}(\kappa c)^6} + \varepsilon\kappa^3\Delta\left(\frac{1}{\kappa^2}, c, \varepsilon\right).$$

Then

$$S_2 = \sqrt{\frac{2}{3}} - \sqrt{\frac{2}{3} - \frac{c^2}{4}\kappa^2 + \frac{1}{24}(\kappa c)^6} + \varepsilon\kappa^3\Delta\left(\frac{1}{\kappa^2}, c, \varepsilon\right),$$

and we observe that $S_2 = \Omega(c, \varepsilon, \kappa)$ with

$$\Omega(c, \varepsilon, \kappa) = \sqrt{\frac{1}{6}}\frac{c^2}{4}\kappa^2 + \kappa^3\Pi(\kappa, c, \varepsilon),$$

for some smooth function Π.

Now applying the transition map $\pi : \Sigma_{in} \to \Sigma_{out}$ in Lemma 4.1 we can track $W^u(1, w_-(\varepsilon))$ to Σ_{out} where it has the expansion

$$r_2 = \kappa,\ T_2 = -\sqrt{\frac{2}{3}} + \phi(\kappa) + \varepsilon\Xi(c, \varepsilon),\ \varepsilon_2 = \varepsilon\Gamma(c, \varepsilon).$$

Remark 4.3. *In theory, all of the analysis required in this section could have been conducted solely in chart K_W as both the relevant fixed points are visible in that chart. However, identifying the heteroclinic connecting the two fixed points is more straightforward in the re-scaling chart K_ε and so we opt to utilize both charts here.*

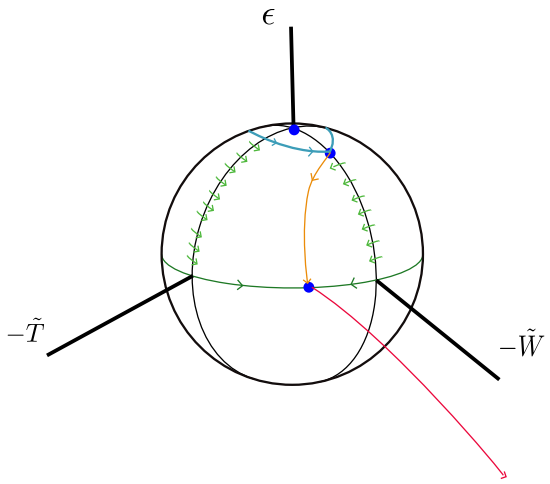

Figure 3: *The relevant dynamics of the blown up fixed point at* $(1, c)$*. The* $\varepsilon = 0$ *subspace is invariant and we have shown the existence of a heteroclinic connecting this fixed point to the origin in Section 3. This is depicted by the red curve. On the upper half of the sphere two fixed points are shown. The one at the north pole is an artificial fixed point that arises when the singularity occurring at* $W = c$ *in (1.4) is removed. The other fixed point corresponds to the steady state* $(1, w_-(0))$*. In the blown-up coordinates this fixed point is hyperbolic and we are able to track its unstable manifold and show that it is heteroclinic to the fixed point at the equator of the sphere. Obtaining estimates on the dynamics for* $0 < \varepsilon \ll 1$ *we are able to show that the unstable manifold of* $(1, w_-(\varepsilon))$ *is* $\mathcal{O}(\varepsilon)$ *close to the reduced heteroclinic shown in red.*

5 Proof of Theorem 1.2

In this section we prove Theorem 1.2 by verifying that the conditions of the Implicit Function Theorem outlined in Theorem 2.1 are satisfied.

By the analysis in the previous section we have that the unstable manifold of $W^u(1, w_-(\varepsilon))$ is well defined and its graph is $\mathcal{O}(\varepsilon)$ close to $(T, g_u(c, T))$. On the other hand, $W^{ss}(0, 0)$ is well defined and depends smoothly on c and ε and for any $0 < T < 1$ is $\mathcal{O}(\varepsilon)$ close to $(T, g_s(c, T))$. Thus, recalling the definition of $\Phi(c, \varepsilon)$ in (2.4) we have

$$\Phi(c, \varepsilon) = g_s\left(c, \frac{1}{2}\right) - g_u\left(c, \frac{1}{2}\right) + \varepsilon R(c, \varepsilon)$$

where $R(c, \varepsilon)$ is smooth.

When $\varepsilon = 0$ and $c^* = \sqrt[3]{\frac{3}{2}}$ then by the analysis presented in Section 3 we have that $\Phi(c^*, 0) = 0$ and furthermore by Lemma 3.1 we have that $\partial_c \Phi(c^*, 0) \neq 0$.

Thus $\Phi(c, \varepsilon)$ satisfies the three conditions set out in Theorem 2.1 necessary for an application of the Implicit Function Theorem. This gives the existence of a smooth function $c^*(\varepsilon)$ such that (1.1) with $\nu = 0$ has a traveling front solution with steep exponential decay that propagates with speed $c = c^*(\varepsilon)$ and for $\rho = \frac{1}{\varepsilon^3}$.

Monotonicity of the front was previously established in [6]. The decay estimate in Theorem 1.2

follows since the front lies in $W^{ss}(0,0)$. This decay rate is specified in (2.3) and after twice re-scaling the independent variable – first to divide the right hand side of the differential equation by a factor of $c - W$ and second to re-scale the independent variable from X to x – then the estimate is obtained.

Acknowledgements

This project was conducted as part of a semester-long undergraduate research project hosted by the Mason Experimental Geometry Lab (MEGL). The research of M.H. was partially supported by the National Science Foundation (DMS-2007759).

References

[1] M. J. Álvarez, A. Ferragut, and X. Jarque. A survey on the blow up technique. *Internat. J. Bifur. Chaos Appl. Sci. Engrg.*, 21(11):3103–3118, 2011.

[2] J. An, C. Henderson, and L. Ryzhik. Pushed, pulled and pushmi-pullyu fronts of the Burgers-FKPP equation, 2021.

[3] M. Avery, M. Holzer, and A. Scheel. Pushed-to-pulled front transitions: continuation, speed scalings, and hidden monotonicity, 2022.

[4] M. Avery and A. Scheel. Universal selection of pulled fronts. *Comm. Amer. Math. Soc.*, 2:172–231, 2022.

[5] J. J. Bramburger and D. Goluskin. Minimum wave speeds in monostable reaction–diffusion equations: sharp bounds by polynomial optimization. *Proceedings of the Royal Society A*, 476(2241):20200450, 2020.

[6] J. J. Bramburger and C. Henderson. The speed of traveling waves in a FKPP-Burgers system. *Arch. Ration. Mech. Anal.*, 241(2):643–681, 2021.

[7] P. Carter and A. Doelman. Traveling stripes in the Klausmeier model of vegetation pattern formation. *SIAM J. Appl. Math.*, 78(6):3213–3237, 2018.

[8] P. Constantin, J.-M. Roquejoffre, L. Ryzhik, and N. Vladimirova. Propagation and quenching in a reactive Burgers-Boussinesq system. *Nonlinearity*, 21(2):221–271, 2008.

[9] G. Dee and J. S. Langer. Propagating pattern selection. *Phys. Rev. Lett.*, 50:383–386, Feb 1983.

[10] F. Dumortier. Techniques in the theory of local bifurcations: blow-up, normal forms, nilpotent bifurcations, singular perturbations. In *Bifurcations and periodic orbits of vector fields*

(Montreal, PQ, 1992), volume 408 of *NATO Adv. Sci. Inst. Ser. C: Math. Phys. Sci.*, pages 19–73. Kluwer Acad. Publ., Dordrecht, 1993.

[11] F. Dumortier, N. Popović, and T. J. Kaper. The critical wave speed for the Fisher-Kolmogorov-Petrowskii-Piscounov equation with cut-off. *Nonlinearity*, 20(4):855–877, 2007.

[12] N. Fenichel. Geometric singular perturbation theory for ordinary differential equations. *J. Differential Equations*, 31(1):53–98, 1979.

[13] I. Gucwa and P. Szmolyan. Geometric singular perturbation analysis of an autocatalator model. *Discrete Contin. Dyn. Syst. Ser. S*, 2(4):783–806, 2009.

[14] K. P. Hadeler and F. Rothe. Travelling fronts in nonlinear diffusion equations. *J. Math. Biol.*, 2(3):251–263, 1975.

[15] K. Harley, P. van Heijster, R. Marangell, G. J. Pettet, and M. Wechselberger. Existence of traveling wave solutions for a model of tumor invasion. *SIAM J. Appl. Dyn. Syst.*, 13(1):366–396, 2014.

[16] M. Holzer and N. Popović. Wavetrain solutions of a reaction-diffusion-advection model of mussel-algae interaction. *SIAM J. Appl. Dyn. Syst.*, 16(1):431–478, 2017.

[17] M. Holzer and A. Scheel. A slow pushed front in a Lotka-Volterra competition model. *Nonlinearity*, 25(7):2151–2179, 2012.

[18] Y. Hosono. Traveling waves for a diffusive Lotka-Volterra competition model. I. Singular perturbations. *Discrete Contin. Dyn. Syst. Ser. B*, 3(1):79–95, 2003.

[19] H. Jardón-Kojakhmetov and C. Kuehn. A survey on the blow-up method for fast-slow systems. In *Mexican mathematicians in the world—trends and recent contributions*, volume 775 of *Contemp. Math.*, pages 115–160. Amer. Math. Soc., [Providence], RI, [2021] ©2021.

[20] C. K. R. T. Jones. Geometric singular perturbation theory. In *Dynamical systems (Montecatini Terme, 1994)*, volume 1609 of *Lecture Notes in Math.*, pages 44–118. Springer, Berlin, 1995.

[21] C. Kuehn. *Multiple time scale dynamics*, volume 191 of *Applied Mathematical Sciences*. Springer, Cham, 2015.

[22] S. Malham and J. X. Xin. Global solutions to a reactive Boussinesq system with front data on an infinite domain. *Comm. Math. Phys.*, 193(2):287–316, 1998.

[23] W. Van Saarloos. Front propagation into unstable states. *Physics reports*, 386(2-6):29–222, 2003.